Journal of Thermal Analysis and Calorimetry, Vol. 92 (2008) 3, 945–951

SYNTHESIS, CHARACTERIZATION AND THERMAL BEHAVIOUR OF SOLID 2-METHOXYBENZOATES OF TRIVALENT METALS

A. B. Siqueira[1,*], *C. T. Carvalho*[1], *E. Y. Ionashiro*[2], *G. Bannach*[2], *E. C. Rodrigues*[3] *and M. Ionashiro*[1]

[1]Instituto de Química, UNESP, CP 355, CEP 14801-970, Araraquara, SP, Brazil
[2]Universidade Estadual de Ponta Grossa, CEP 84010-919, Ponta Grossa, PR, Brazil
[3]Fundação Educacional de Barretos, CEP 14780-000, Barretos, SP, Brazil

Solid-state $Ln(L)_3$ compounds, where *Ln* stands for trivalent Eu, Gd, Tb, Dy, Ho, Er, Tm, Yb, Lu and Y and *L* is 2-methoxybenzoate have been synthesized. Simultaneous thermogravimetry and differential thermal analysis (TG-DTA), differential scanning calorimetry (DSC), X-ray powder diffractometry, infrared spectroscopy and complexometry were used to characterize and to study the thermal behaviour of these compounds. The results provided information on the composition, dehydration, coordination mode, structure, thermal behaviour and thermal decomposition.

Keywords: *characterization, heavier lanthanides, 2-methoxybenzoate, thermal behaviour*

Introduction

Several metal-ion compounds of benzoate, C_6H_5–COO^- (Bz), and phenyl-substituted derivatives of benzoate have been investigated in aqueous solutions [1–3] and in solid state [4–13]. In aqueous solutions these works reported the thermodynamics of complexation of lanthanides by some benzoic acid derivatives; the spectroscopic study of trivalent lanthanides with several carboxylic acids including benzoic acid; the influence of pH, surfactant and synergic agent on the luminescent properties of terbium chelates with benzoic acid derivatives and thermodynamic of complexation of lanthanides by benzoic and isophthalic acids [1–3].

In solid state the works reported the thermal and spectral studies on solid compounds of benzoate and derivatives with rare earth elements; the reaction of divalent copper, cobalt and nickel with 3-hydroxy-4-methoxy and 3-methoxy-4-hydroxybenzoic acid and structure for these compounds has been proposed on the basis of spectroscopic and thermogravimetric data; the thermal decomposition of thorium salts of benzoic and 4-methoxybenzoic acids in air atmosphere and thermal behaviour of solid state methoxybenzoate of some divalent transition metal ions [4–13].

In this work 2-methoxybenzoates of trivalent Eu, Gd, Tb, Dy, Ho, Er, Tm, Yb, Lu and Y were synthesized. The compounds were investigated by means of infrared spectroscopy, X-ray powder diffractometry, simultaneous thermogravimetry and differential thermal analysis (TG-DTA), differential scanning calorimetry (DSC) and other methods of analysis.

Experimental

Materials

The 2-methoxybenzoic acid (*HL*) 99% was obtained from Aldrich. Aqueous solution of Na–L 0.15 mol L^{-1} was prepared from aqueous HL suspension by treatment with sodium hydroxide solution (0.1 mol L^{-1}). Lanthanide chlorides were prepared from the corresponding metal oxides by treatment with concentrated hydrochloric acid. The resulting solutions were evaporated to near dryness, the residues were again dissolved in distilled water, transferred to a volumetric flask and diluted in order to obtain ca. 0.1 mol L^{-1} solutions, whose pH were adjusted to 5.0 by adding diluted sodium hydroxide or hydrochloric acid solutions. The solid state compounds were prepared by adding slowly, with continuous stirring the ligand solution to the respective metal chloride solutions, until total precipitation of the metal ions. The precipitates were washed with distilled water until elimination of the chloride ions, filtered through and dried on Whatman n° 42, filter paper, and kept in a desiccator over anhydrous calcium chloride.

In the solid-state compounds, hydrate water, ligand and metal ion contents were determined from the TG curves. The metal ions were also determined by complexometric titrations with standard EDTA

---

* Author for correspondence: massaoi@yahoo.com.br

1388–6150/$20.00

Akadémiai Kiadó, Budapest, Hungary
Springer, Dordrecht, The Netherlands

Table 1 Analytical and thermoanalytical (TG) data of the compounds

Compound	Metal/%			ΔL/%		H_2O/%		C%		H%		Final Residue
	Calcd.	TG	EDTA	Calcd.	TG	Calcd.	TG	Calcd.	AE	Calcd.	AE	
$Eu(L)_3{\cdot}3H_2O$	23.05	22.27	23.47	65.12	65.00	8.19	8.49	43.71	43.63	4.13	4.28	Eu_2O_3
$Gd(L)_3{\cdot}4H_2O$	23.03	23.27	23.33	62.90	62.77	10.56	10.70	42.22	42.13	4.29	4.32	Gd_2O_3
$Tb(L)_3{\cdot}4H_2O$	23.22	23.99	23.02	62.16	61.53	10.53	10.29	42.11	41.68	4.28	4.23	Tb_4O_7
$Dy(L)_3{\cdot}5H_2O$	23.01	22.87	23.42	60.82	61.03	12.76	12.58	40.82	40.96	4.43	4.45	Dy_2O_3
$Ho(L)_3{\cdot}3.5H_2O$	24.14	24.33	24.20	63.02	62.54	9.25	9.48	42.30	41.98	4.15	4.11	Ho_2O_3
$Er(L)_3{\cdot}H_2O$	26.19	26.32	26.42	67.27	67.04	2.82	2.66	41.60	41.45	4.23	4.21	Er_2O_3
$Tm(L)_3{\cdot}H_2O$	26.38	26.76	26.75	67.06	66.80	2.81	2.93	45.01	44.83	3.63	3.67	Tm_2O_3
$Yb(L)_3{\cdot}H_2O$	26.87	27.22	27.39	66.70	66.35	2.80	2.71	44.72	44.43	3.60	3.63	Yb_2O_3
$Lu(L)_3{\cdot}H_2O$	27.07	27.60	27.64	66.43	65.94	2.79	2.71	44.62	44.56	3.59	3.65	Lu_2O_3
$Y(L)_3{\cdot}4H_2O$	14.47	14.77	14.56	69.89	69.78	11.73	11.46	47.05	47.93	4.78	4.63	Y_2O_3

L=2-methoxybenzoate

solution using xylenol orange as indicator [14, 15]. X-ray powder patterns were obtained by using a Siemens D-5000 X-ray diffractometer, employing CuK_α radiation (λ=1.541 Å) and setting of 40 kV and 20 mA.

Infrared spectra for Na–2-MeO–Bz as well as for its metal-ion compounds were recorded on a Nicolet model Impact 400 FT-IR instrument, within the 4000–400 cm^{-1} range. The solid samples were pressed into KBr pellets.

Simultaneous TG-DTA and DSC curves were obtained with two thermal analysis systems, model SDT 2960 and DSC Q10, both from TA Instruments. The purge gas was an air with a flow rate of 100 mL min^{-1} for TG-DTA and 50 mL min^{-1} for DSC experiments. A heating rate of 20°C min^{-1} was adopted, with sample masses about 7 mg for TG-DTA and 5 mg for DSC runs. Alumina and aluminium crucibles, the latter with perforated covers, were used for TG-DTA and DSC, respectively.

Computational strategy

Calculation of theoretical infrared spectrum of yttrium 2-methoxibenzoate was necessary to evaluate the structure and wave function computed by the ab initio SCF Hartree-Fock-Roothan method [16] using a split valence (cep-31 g) basis set [17]. The performed molecular calculations in this work were done by using the Gaussian 98 routine [18] and the hardware IBM power 3. The geometry optimization was carried out without any constraints. The benzoate molecule contains rings with conformational flexibility, and all variables optimized. The optimization proceeded more uniformly when all variables were optimized.

Results and discussion

The analytical and thermoanalytical (TG) data are shown in Table 1. These results establish the stoichiometry of these compounds, which are in agreement with the general formula $Ln(L){\cdot}nH_2O$, where Ln represents trivalent Eu to Lu or Y, L is 2-methoxybenzoate and n=5 (Dy), 4 (Gd, Tb, Y), 3.5 (Ho), 3 (Eu), 1 (Er, Tm, Yb, Lu).

The X-ray diffraction powder patterns (Fig. 1) show that all the compounds have a crystalline structure without evidence for formation of an isomorphous series, except for ytterbium and lutetium compounds which are isomorphous.

Infrared spectroscopic data on 2-methoxybenzoate and its compounds with trivalent metal ions considered in this work are shown in Table 2. The investigation

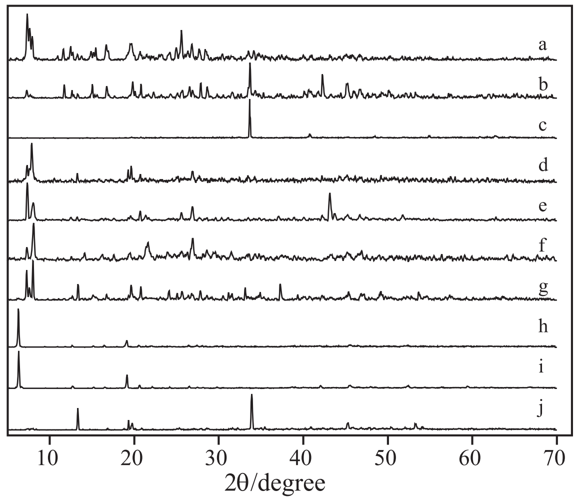

Fig. 1 X-ray powder diffraction patterns of the compounds: a – $Eu(L)_3{\cdot}H_2O$; b – $Gd(L)_3{\cdot}4H_2O$; c – $Tb(L)_3{\cdot}4H_2O$; d – $Dy(L)_3{\cdot}5H_2O$; e – $Ho(L)_3{\cdot}3.5H_2O$; f – $Er(L)_3{\cdot}1H_2O$; g – $Tm(L)_3{\cdot}1H_2O$; h – $Yb(L)_3{\cdot}1H_2O$; i $Lu(L)_3{\cdot}1H_2O$; j – $Y(L)_3{\cdot}4H_2O$. L=2-methoxybenzoate

Table 2 Spectroscopic data (cm^{-1}) taken from IR spectra for sodium 2-methoxybenzoate and compounds with europium(III), heavy lanthanides(III) and yttrium(III)

Compound	$\nu_{(O–H)}H_2O^b$	$\nu_{asym(COO^-)}^c$	$\nu_{sym(COO^-)}^c$	$\Delta\nu(\nu_{asym}–\nu_{sym})$
NaL	–	1576_s	1404_s	172
$Eu(L)_3·3H_2O$	3479_m	1537_s	1402_s	135
$Gd(L)_3·4H_2O$	3487_m	1547_s	1398_s	149
$Tb(L)_3·4H_2O$	3489_m	1548_s	1402_s	146
$Dy(L)_3·5H_2O$	3489_m	1547_s	1404_s	143
$Ho(L)_3·3.5H_2O$	3481_m	1548_s	1404_s	144
$Er(L)_3·H_2O$	3483_m	1549_s	1406_s	143
$Tm(L)_3·H_2O$	3466_m	1549_s	1420_s	129
$Yb(L)_3·H_2O$	3471_m	1549_s	1418_s	131
$Lu(L)_3·H_2O$	3504_m	1553_s	1419_s	134
$Y(L)_3·4H_2O$	3485_m	1553_s	1402_s	151

L=2-methoxybenzoate; [a]m – medium; s – strong; [b]$\nu_{(O–H)}$: hydroxyl group stretching frequency; [c]$\nu_{asym(COO^-)}$ and $\nu_{sym(COO^-)}$: symmetrical and antisymmetrical vibrations of the COO^- group, respectively

Table 3 Theoretical geometrical parameters of $Y(L)_3$ compound

$dY–{}^aO_{COO^-}$	2.35 Å
$dY–{}^bO_{COO^-}$	2.33 Å
$dC_{COO^-}–{}^aO_{COO^-}$	1.29 Å
$dC_{COO^-}–{}^bO_{COO^-}$	1.31 Å
$dC_{COO^-}–C_{ring}$	1.48 Å
$dO_{OCH_3}–C_{OCH_3}$	1.44 Å
$dC_{ring}–O_{OCH_3}$	1.36 Å
$dC_{OCH_3}–H_{OCH_3}$	1.08 Å
$dC_{ring}–H_{ring}$	1.07 Å
$<O_{COO^-}–C_{COO^-}–O_{COO^-}$	114.96°
$<O_{COO^-}–Y–O_{COO^-}$	55.76°
$<C_{ring}–O_{OCH_3}–C_{OCH_3}$	122.10°

Key: Y=yttrium; *L*=2-methoxybenzoate; d=atomic distances; <=angle of atoms; CO^aO^{b-}=carboxylate; ring=benzene ring; OCH_3=methoxy group

was focused mainly within the 1700–1400 cm^{-1} range because this region is potentially the most informative to assign coordination sites. In the sodium 2-methoxybenzoate strong bands located at 1576 and 1404 cm^{-1} are attributed to the anti-symmetrical and symmetrical frequencies of the carboxylate groups, respectively [19–21]. For the synthesized compounds, the anti-symmetrical and symmetrical stretching frequencies are located between 1553–1537 and 1420–1398 cm^{-1}, respectively. Analysis of the frequencies of the $\nu_{as(COO^-)}$ and $\nu_{sym(COO^-)}$ bands shows that the lanthanides are linked to the carboxylate group by a bidentate bond with an incomplete equalization of bond lengths in the carboxylate anion, which is in agreement with [22].

The theoretical infrared spectrum of the $Y(L)_3$ was calculated by using a harmonic field [23] and the obtained frequencies were not scaled. The geometry optimization was computed by the optimized algorithm of Berny [23]. The obtained geometry from calculations is presented in Table 3.

The theoretical infrared spectrum of the $Y(L)_3$ (electronic state ^1A) was obtained with frequency values (cm^{-1}), relative intensities, assignments and description of vibrational modes. The theoretical frequency, assignments and description was visualized by using graphic software Molden 4.2 for Linux [24]. It was compared to the experimental infrared spectrum of $Y–(2\text{-}MeO–Bz)_3$.

A comparative analysis between the experimental and theoretical spectrum permitted to verify that: (a) the first assignment shows a strong contribution at 1553 cm^{-1} suggesting a $\nu_{asym(COO^-)}$ assignment, while the theoretical results show the corresponding peak at 1558 cm^{-1} with discrepancies of 0.32%; (b) the second assignment shows a strong contribution at 1402 cm^{-1} suggesting a $\nu_{sym(COO^-)}$ assignment, while the theoretical results show the corresponding peak at 1378 cm^{-1} with discrepancies of 1.71%. The theoretical results are in agreement with the experimental data.

Simultaneous TG-DTA curves of the compounds show mass losses in steps and thermal events corresponding to these losses or due to physical phenomenon.

Due to the great similarity in the thermoanalytical curves, consequently in the thermal behaviors, only the TG-DTA curves of europium, dysprosium, thulium and lutetium compounds are shown in Fig. 2.

For all the compounds, the first mass loss between 313–383 K with endothermic peaks at 363–383 K is attributed to the dehydration, which occurs in a single step. Once dehydrated, the TG-DTA curves also show

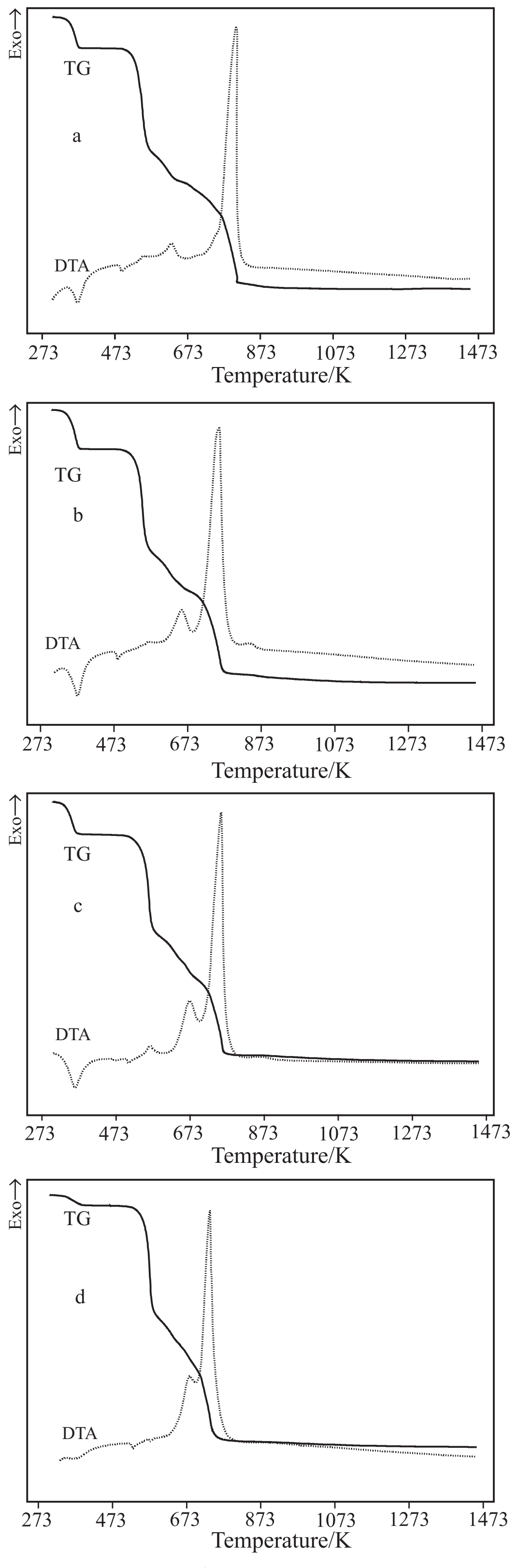

Fig. 2 TG-DTA curves of a – $Eu(L)_3{\cdot}3H_2O$ (m=7.246 mg); b – $Dy(L)_3{\cdot}5H_2O$ (m=6.913 mg); c – $Tm(L)_3{\cdot}H_2O$ (m=7.010 mg); d – $Lu(L)_3{\cdot}H_2O$ (m=6.657 mg); L=2-methoxybenzoate

that the anhydrous compounds are stable up to 493 K (Eu to Ho and Y), 503 K (Er, Tm), and 523 K (Yb, Lu) and above this temperature up to 818 K (Eu), 783 K (Gd, Dy, Y), 798 K (Tb), 773 K (Ho, Er, Tm, Lu) and 753 K (Yb), the mass losses occur in three steps without a plateau between the steps. In correspondence with the mass losses, the DTA curve shows for the first step a small and broad exothermic and/or endothermic events attributed to the thermal decomposition (endo) together the oxidation of evolved products (exo), where the resulting net heats produce only small thermal event. For the two last mass losses, the exothermic peaks are attributed to oxidation of the organic matter.

For all the compounds, the TG curve shows that the mass loss in the last step occurs through a slow process, corresponding to a small and broad exothermic events (Gd, Dy–Tm, Y) or without thermal events (Eu, Tb, Yb, Lu). Tests with hydrochloric acid solution on samples heated up to the initial temperature of the last step, as indicated by the corresponding TG curves, showed in all cases, the presence of carbonaceous residue and evolution of CO_2 (except terbium). The formation of dioxycarbonate as intermediate, has already been observed during the thermal decomposition of other lanthanide compounds [12, 13]. For the terbium compound the thermal decomposition occurs without formation of the intermediate, probably due to oxidation of Tb(III) to Tb_4O_7 (exo), together the oxidation of the organic matter (exo).

Calculations based on the mass loss observed in this step of the TG curve, suggest the formation of a mixture of lanthanide oxide (Ln_2O_3) and lanthanide dioxycarbonate $Ln_2O_2CO_3$, in no simple stoichiometric relation. Thus, the last step is attributed to oxidation of the carbonaceous residue and thermal decomposition of the dioxycarbonate (except terbium), to the respective oxide, Tb_4O_7 or Ln_2O_3 (Ln=Eu, Gd, Dy to Lu and Y).

The mass losses, temperature ranges and the peak temperatures observed for each step of the TG-DTA curves are shown in Table 4.

In all the compounds, the endothermic peak at 491 K (Eu), 492 K (Gd), 483 K (Tb, Dy), 485 K (Ho, Er) and 490 K (Y) without mass loss in the TG curves is attributed to the phase transition. For the thulium, ytterbium and lutetium compounds the endothermic peak at 473, 522 and 527 K, respectively, is attributed to the phase transition, which occurs simultaneously with the beginning of thermal decomposition of the anhydrous compound. The phase transition was also observed during the thermal decomposition of lanthanide 4-methoxybenzoate [12, 13].

A great similarity is also observed in the DSC profiles of these compounds, therefore only the DSC curves of europium, dysprosium, ytterbium and

Table 4 Temperature ranges θ, mass losses (%) and peak temperatures observed for each step of TG-DTA curves of the compounds

Compound		Steps					Phase transition
		first	second	third	fourth	fifth	
$Eu(L)_3·3H_2O$	θ K	313–383	493–573	573–673	673–818	818–1073	
	loss/%	8.19	26.95	9.51	26.95	1.59	
	peak/K	371 (endo)	550 (exo)	629 (exo)	807 (exo)	–	491 (endo)
$Gd(L)_3·4H_2O$	θ K	313–383	493–578	578–688	688–783	783–1073	
	loss/%	10.56	27.36	6.44	26.82	2.15	
	peak/K	377 (endo)	558 (exo)	652 (exo)	772 (exo)	863 (exo)	492 (endo)
$Tb(L)_3·4H_2O$	θ K	313–383	493–573	573–683	683–798	798–1173	
	loss/%	10.53	26.15	9.74	23.85	1.79	
	peak/K	377 (endo)	–	656 (exo)	785 (exo)	–	483 (endo)
$Dy(L)_3·5H_2O$	θ K	313–383	493–573	573–683	683–783	793–1173	
	loss/%	12.76	26.67	10.77	21.03	2.56	
	peak/K	373 (endo)	563 (exo)	663 (exo)	768 (exo)	853 (exo)	483 (endo)
$Ho(L)_3·3.5H_2O$	θ K	323–383	493–578	578–683	683–773	773–1173	
	loss/%	9.25	27.10	10.94	22.41	2.09	
	peak/K	366 (endo)	561 (exo)	662 (exo)	750 (exo)	863 (exo)	485 (endo)
$Er(L)_3·H_2O$	θ K	323–383	503–578	578–693	693–773	773–1173	
	loss/%	2.82	28.34	14.17	22.35	2.18	
	peak/K	383 (endo)	559 (endo)	667 (exo)	759 (exo)	883 (exo)	485 (endo)
$Tm(L)_3·H_2O$	θ K	323–383	503–578	578–703	703–773	773–1173	
	loss/%	2.81	27.88	15.68	20.91	2.33	
	peak/K	363 (endo)	568 (exo)	669 (exo)	757 (exo)	873 (exo)	506 (endo)
$Yb(L)_3·H_2O$	θ K	323–383	523–593	593–693	693–753	753–1073	
	loss/%	2.80	28.25	16.42	17.74	3.94	
	peak/K	373 (endo)	571 (endo)	667 (exo)	733 (exo)	–	522 (endo)
$Lu(L)_3·H_2O$	θ K	323–383	523–593	593–698	698–773	773–1173	
	loss/%	2.79	30.07	14.77	19.52	1.58	
	peak/K	382 (endo)	576 (endo)	680 (exo)	736 (exo)	–	527 (endo)
$Y(L)_3·4H_2O$	θ K	313–383	493–578	578–693	693–783	783–1173	
	loss/%	11.73	30.00	13.04	24.46	2.28	
	peak/K	365 (endo)	577 (endo)	665 (exo)	771 (exo)	883 (exo)	490 (endo)

L=2-methoxybenzoate

yttrium compounds are shown in Fig. 3. These curves show endothermic and exothermic events that all accord with the mass losses observed in the TG curves and endothermic peaks due to crystalline phase transition. The first endothermic peak observed between 361 and 380 K is attributed to dehydration and in agreement with the TG-DTA curves.

The second endothermic peak at 493 K (Eu, Gd), 486 K (Tb), 483 K (Dy), 485 K (Ho), 487 K (Er), 508 K (Tm), 520 K (Yb), 530 K (Lu) and 492 K (Y) is attributed to the reversible phase transition as it can be seen in the DSC curve of the holmium compound, Fig. 4 as representative for all the compounds. The reversible phase transition had already been observed in the other lanthanide compounds [12, 13]. The third endothermic peak at 551 K (Eu, Gd, Tb), 552 K (Dy), 555 K (Ho), 557 K (Er), 564 K (Tm), 569 K (Yb), 576 K (Lu) and 561 K (Y) is ascribed to the first step of thermal decomposition of the anhydrous compound

Table 5 Enthalpies in kJ mol^{-1} found for dehydration (A), reversible phase transition (B) and elimination of 2-methoxybenzoic anhydride (C) of the synthesized compounds

Compound	A	B	C
$Eu(L)_3·3H_2O$	142.4	32.4	26.7
$Gd(L)_3·4H_2O$	214.4	32.9	30.3
$Tb(L)_3·4H_2O$	165.4	38.3	33.8
$Dy(L)_3·5H_2O$	230.9	36.0	29.1
$Ho(L)_3·3.5H_2O$	188.9	34.4	31.7
$Er(L)_3·H_2O$	47.5	34.8	37.1
$Tm(L)_3·H_2O$	43.2	17.3	21.5
$Yb(L)_3·H_2O$	42.0	23.7	34.8
$Lu(L)_3·H_2O$	38.9	20.1	31.1
$Y(L)_3·4H_2O$	113.5	20.7	27.6

L=2-methoxybenzoate

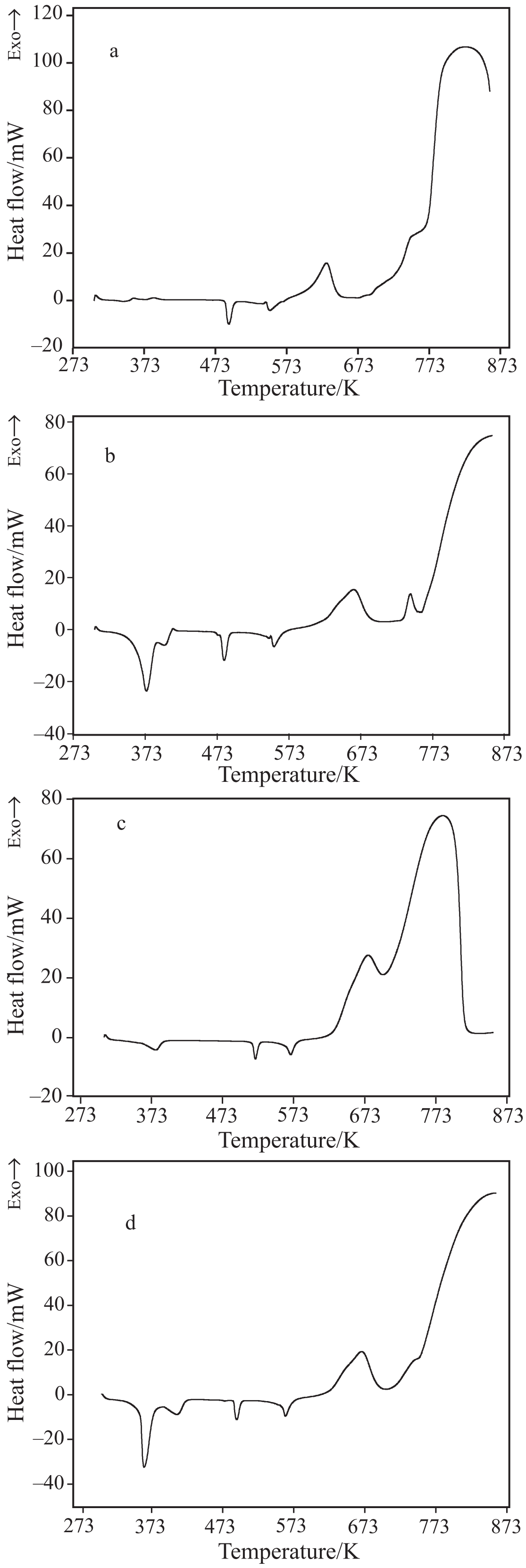

Fig. 3 DSC curves of the a – Eu(L)$_3$·3H$_2$O (m=4.530 mg); b – Dy(L)$_3$·5H$_2$O (m=5.123 mg); c – Yb(L)$_3$·H$_2$O (m=4.805 mg); d – Y(L)$_3$·4H$_2$O (m=5.001 mg); L=2-methoxybenzoate

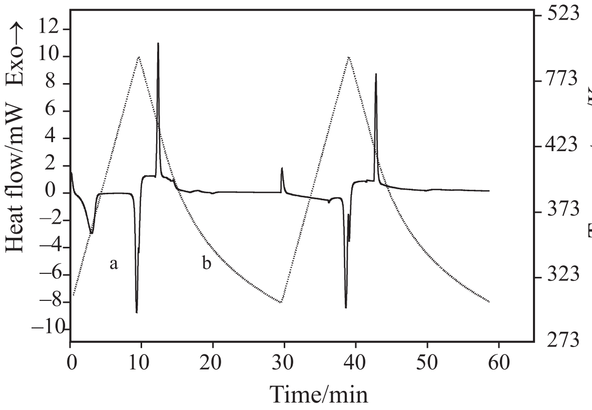

Fig. 4 DSC curves on a – heating and b – cooling of the Ho (L)$_3$·3.5H$_2$O (L=2-methoxybenzoate) compound

with elimination of 2-methoxybenzoic anhydride. Tests with samples heated in a glass tube up to the temperature indicated by the DSC curves showed in all cases the formation of sublimate material and the analysis of this material confirmed to be the 2-methoxybenzoic anhydride.

The exothermic events above 573 K (Eu) and 623 K (Gd–Lu, Y) are attributed to the thermal decomposition of the anhydrous compounds where the oxidation of the organic matter takes place in consecutive and/or overlapping steps.

The enthalpies belonging to dehydration, reversible phase transition and elimination of 2-methoxybenzoic anhydride are shown in Table 5.

Conclusions

From TG curves and complexometry results, a general formula could be established for these compounds in the solid state.

The X-ray powder patterns pointed out that the synthesized compounds have a crystalline structure without evidence concerning to the formation of isomorphous series, except the ytterbium and lutetium compounds.

The experimental and theoretical infrared spectroscopy data suggest that 2-methoxybenzoate acts as a bidentate bond with an incomplete equalization of bond lenghts in the carboxylate anion.

The TG-DTA and DSC curves provided previously underported information concerning the thermal behaviour and thermal decomposition of these compounds.

Acknowledgements

The authors thank FAPESP (Proc. 97/12646-8), CNPq and CAPES Foundation (Brazil) for financial support and computational facilities of IQ-UNESP and CENAPAD-UNICAMP.

References

1 S. J. Yun, S. K. Kang and S. S. Yun, Thermochim. Acta, 331 (1999)13.
2 Z. M. Wang, L. J. Van de Burgt and G. R. Choppin, Inorg. Chim. Acta, 167 (1999) 293.
3 N. Arnaud and J. Georges, Analyst, 125 (2000) 1487.
4 G. R. Choppin, O. Liu and E. N. Rizkalla, Inorg. Chim. Acta, 145 (1988) 309.
5 W. Ferenc and B. Bocian, J. Therm. Anal. Cal., 74 (2003) 521.
6 W. Brzyska and W. Ozga, J. Therm. Anal. Cal., 78 (2004) 999.
7 W. Ferenc and A. Walkow-Dziewulska, J. Therm. Anal. Cal., 71 (2003) 375.
8 A. Kula, J. Therm. Anal. Cal., 81 (2005) 381.
9 E. C. Rodrigues, A. B. Siqueira, E. Y. Ionashiro, G. Bannach and M. Ionashiro, J. Therm. Anal. Cal., 79 (2005) 323.
10 A. C. Vallejo, A. B. Siqueira, E. C. Rodrigues, E. Y. Ionashiro, G. Bannach and M. Ionashiro, Ecl. Quim., 30 (2005) 7.
11 C. T. Carvalho, A. B. Siqueira, E. C. Rodrigues and M. Ionashiro, Ecl. Quim., 30 (2005) 19.
12 E. C. Rodrigues, A. B. Siqueira, E Y Ionashiro, G. Bannach and M. Ionashiro, Ecl. Quím., 31 (2006) 21.
13 E. C. Rodrigues, A. B. Siqueira, E. Y. Ionashiro, G. Bannach and M. Ionashiro, Thermochim. Acta, 451 (2006) 149.
14 H. A. Flaschka, EDTA Titrations, Pergamon Press, Oxford 1964.
15 M. Ionashiro, C. A. F. Graner and J. Zuanon Netto, Ecl. Quim., 8 (1983) 29.
16 21. C. C. J. Roothaan, Rev. Mod. Phys., 23 (1951) 69.
17 W. J. Stevens, M. Krauss, H. Basch and P. G. Jasien, Can. J. Chem., 70 (1992) 612.
18 K. D. Dobbs and W. J. Hehre, J. Comput. Chem., 8 (1987) 880.
19 G. Socrates, Infrared Characteristic Group Frequencies, 2nd Ed., Wiley, New York 1994, pp. 91 and 236–237.
20 R. M. Silverstein and F. X. Webster, Spectrometric Identification of Organic Compounds, Wiley, New York, 6th Ed., pp. 92, 93, 96 and 97.
21 M. Kalinowska, R. Swistocka and W. Lewandowski, J. Mol. Struct., 792 (2006) 130.
22 W. Lewandowski and H. Baranska, J. Raman Spectrosc., 17 (1986) 17.
23 D. Z. Goodson, J. Phys. Chem., 86 (1998) 659.
24 Schaftenaar, G.; Molden 4.2; CAOS/CAMM Center Nijmegen Toernooiveld, Holanda 1991.

Received: May 3, 2007
Accepted: October 2, 2007

DOI: 10.1007/s10973-007-8546-1